Journal of Applied Polymer Science

Synthesis and Characterization of Secondary Doped Polypyrrole/Organic Modified Attapulgite Conductive Composites

Huixia Feng,[1] Bin Wang,[1] Nuoxin Wang,[2,3] Jianhui Qiu,[4] Lin Tan,[1] Nali Chen[1]

[1]College of Petrochemical Technology, Lanzhou University of Technology, Lanzhou 730050, People's Republic of China
[2]School of Life Science and Technology, Harbin Institute of Technology, Harbin 150080, People's Republic of China
[3]CAS Key Lab of Biological Effects of Nanomaterials and Nanosaftey, National Center of Nanoscience and Technology, Beijing 100190, People's Republic of China
[4]Department of Machine Intelligence and Systems Engineering Faculty of Systems Engineering, Akita Prefectural University, Akita 015-0055, Japan
Correspondence to: H. Feng (E-mail: fenghx66@163.com)

ABSTRACT: Secondary doping method was introduced into fabricating polypyrrole/oganic modified attapulgite conductive composites. The preparation conditions, such as amount of hexadecylpyridinium chloride (CPC, modifying agent), organic modified attapulgite (OATP), and HCl (secondary dopant) have been optimized to get the composites with the highest conductivity. When m_{CPC}/m_{ATP}, m_{OATP}/m_{Py}, and n_{HCl}/n_{SA} (SA is sulfamic acid) reaches 0.03, 0.6, and 0.5, respectively, the PPy/OATP composites possess the highest conductivity of 87.59 S cm^{-1} as well as the highest thermal degradation temperature of 249.29°C. Scanning electron microscopy, transmission electron microscopy, X-ray diffraction, Fourier transform infrared spectroscopy, UV-Visible diffuse reflectance study, and X-ray photoelectron Spectroscopy results showed that PPy chains form the core-shell structure and may combine with OATP via π–π stacking interaction. Thermogravimetric analysis showed that the thermal stability of PPy/OATP-SH composites was enhanced and these could be attributed to the retardation effect of OATP as barriers for the degradation of PPy. This method may open a new door for PPy-based composites with special structures, higher performance, and thus broader application ranges. © 2014 Wiley Periodicals, Inc. J. Appl. Polym. Sci. **2015**, *132*, 41407.

KEYWORDS: clay; composites; conducting polymers

Received 28 April 2014; accepted 15 August 2014
DOI: 10.1002/app.41407

INTRODUCTION

Recently, conducting polymers have attracted increasingly growing attention in material science. Among them, PPy has been broadly used in electronic devices,[1] biomedical tests,[2] and chemical sensors[3] for its good conductivity as well as thermal and light stability in air atmosphere. However, its conductivity, as any other eigenstates conductive polymers, is still rather low for the further ultilization.[4] Inspiringly, many researches have showed that the acid dopant could enlarge the conductivity of PPy.[5–7] Bay and co-workers compared the conductivity of PPy doped by different alkyl benzenesulfonates. The results indicate that the highest electronic conductivity (83 S cm^{-1}) is found for p-(n-butyl) benzenesulfonate doped PPy.[6] He et al. chose dodecyl-benzene sulfonic acid (DBSA) as dopant and prepared PPy, the results showed that the highest conductivity (43.18 S cm^{-1}) is found when the concentration of DBSA is 0.18*M*.[8]

Although PPy possesses improved conductivity under its doped form, it is still insoluble, infusible, and brittle, thereby greatly limiting its processability.[9] To solve these problems, recently, inorganic nano-materials were widely introduced to construct PPy-based composites, by which we could obtain composites with not only better mechanical strength and solubility but even enhanced conductivity to some extent.[10–12] For example, Dubey and co-workers have synthesized poly(benzothiadiazole)/carbon nanotube (CNT) composites and found their conductivity depends on the concentration of CNT in polymer, the highest conductivity of composites is 440 S cm^{-1} when CNT 10 wt %[13]; Mallouki has prepared PPy/Fe_2O_3 composites and conductivity of composites could reach 56.6 S cm^{-1} when Fe_2O_3 takes up 41.86 wt %.[14] From these examples, we can find that the dose of inorganic dopants is a key parameter in the composites.

Attapulgite (ATP) is a kind of crystalline hydrated magnesium aluminum silicate with unique fibrous three-dimensional structure.

© 2014 Wiley Periodicals, Inc.

Table I. The Preparation Conditions of OATP

Samples	ATP (g)	m_{CPC}/m_{ATP}[a]	CPC (g)
OATP1	4	0.01	0.04
OATP2	4	0.02	0.08
OATP3	4	0.025	0.1
OATP4	4	0.03	0.12
OATP5	4	0.035	0.14

[a] The mass ratio of CPC and ATP.

ATP has many advantages compared with other nature minerals for preparation of conductive polymer/organic modified ATP composites: (a) many reactive-OH groups lie on ATP surfaces and it benefits surfactant modification; (b) the fibrous morphology of ATP benefits to forming the conductive spliced network; and (c) it has a large surface area and thus strong absorptive capacity.[15] Some researchers have got the organic modified ATP and then prepared the PPy/organic modified attapulgite (OATP) composites. For example, Yang et al got the organic modified OATP by γ-aminopropyltriethoxysilane and then prepared the PPy/OATP composites. This sample had the highest conductivity (50 S cm^{-1}) and the onset decomposition temperatures of composites were higher than that of PPy, which also shifts towards the higher temperature range as the content of OATP increased.[16]

In this paper, we report a facile method to synthesize PPy/OATP composites with well-defined structures. For this, first, the OATP was prepared by the self-assembly of CPC (organic modifier) on the surfaces of ATP. Second, OATP was dispersing in pyrrole (Py) suspension and Py was absorbed on the surface of OATP with the help of the terminal pyridine groups of OATP surface by π–π stacking interaction. At last, PPy/OATP composites were prepared in aqueous solution by *in situ* polymerizing Py. Interestingly, we find that the conductivity of the composites could be further improved when we introduced HCl as the secondary dopant following the SA as the initial one in the process of polymerization. Because of the critical impact of the dopant ratio on composite conductivity, optimization experiments have been made to figure out the maximum conductivity of PPy/OATP composites by changing the amount of CPC, OATP, and HCl. It is indicated that the highest conductivity of these prepared composites reaches 87.59 S cm^{-1}, 3.7 times larger than that of pure PPy. The characterization results show that the OATP nanoparticles are well covered by PPy chains and form the core-shell structures; the thermal stability of composites are greatly enhanced when introduced OATP as well.

EXPERIMENTAL

Materials

Py monomer was purified by distillation under reduced pressure. ATP ultrafine powder with the average diameter of 325 mesh and purity of 99.5% (Xuyi Colloidal, Jiangsu, China), it was calcined at 350°C for 2 h, followed by a treatment with 1*M* hydrochloric acid for 4 h, washed with distilled water until pH = 7, and dried in vacuum at 50°C for 12 h before use. Other reagents (all are locally commercially available and of analytical grade), such as SA, CPC, and $FeCl_3$, were used without further purification. All solutions were prepared with distilled water.

Preparation of Organic Modified Attapulgite

ATP was organic modified using CPC. Typically, 0.12 g CPC was dissolved in 100 mL deionized water and 4.00 g ATP powder was added. The reaction mixture was vigorously stirred at room temperature for 4 h. The resulting solution was filtered and repeatedly washed with deionized water to remove other reagents. The product was dried in a vacuum oven at 50°C for 12 h to get OATP powder. The condition of the OATP preparation is given in Table I.

Preparation of PPy

PPy was prepared by chemical oxidation. One mL Py monomer was dispersed in 50 mL distilled water at ambient temperature. Then, under nitrogen protection, 1.118 g sulfamic acid (SA) and 50 mL 0.3*M* $FeCl_3$ solution was added slowly to the mixture. After magnetic stirring for 0.5 h, the resultant product was dried under vacuum at 40°C for 12 h to obtain a black powder of PPy.

Preparation of PPy/SA-Doped OATP Composites

The PPy/SA-doped OATP (OATP-S) composites were prepared by *in situ* chemical oxidative polymerization method. In a typical process, 0.58 g OATP and 1.118 g SA were added in 50.00 mL deionized water and stirred at room temperature for 4 h, and then 1 mL Py was added into the mixture with vigorous stirring. Afterward, 50.00 mL 0.30*M* $FeCl_3$ solution was added drop by drop to the above mixture to start the polymerization. The reaction was performed under nitrogen protection for 0.5 h. Finally, the product was removed from solution, copiously washed with deionized water and dried in vacuum at 50°C for 12 h to obtain of the PPy/OATP-S composites as a black powder. The condition of the PPy/OATP-S preparation is given in Table II.

Preparation of HCl Secondary Doped PPy/OATP Composites

We also introduced secondary doping method in the polymerization process to compare with the polymerization which only be doped once by SA. The HCl secondary doped PPy/OATP (PPy/OAYP-SH) composites were fabricated the same as the PPy/OATP-S except that certain volume of 1*M* HCl solution was added 15 min later from beginning polymerization. The condition of the PPy/OATP-SH preparation is given in Table III.

Table II. The Preparation Conditions of PPy/OATP-S Composites

Samples	Py (mL)	m_{OATP}/m_{Py} [a]	OATP (g)
PPy/OATP-S1	1	0.4	0.39
PPy/OATP-S2	1	0.6	0.58
PPy/OATP-S3	1	0.8	0.78
PPy/OATP-S4	1	1.2	1.16
PPy/OATP-S5	1	1.6	1.55
PPy/OATP-S6	1	2.0	1.94

[a] The mass ratio of OATP and Py.

Table III. The Preparation Conditions of PPy/OATP-SH Composites

Samples	Py (mL)	n_{HCl}/n_{SA} [a]	1*M* HCl (mL)
PPy/OATP-SH1	1	0.1	1.15
PPy/OATP-SH2	1	0.3	3.45
PPy/OATP-SH3	1	0.5	5.76
PPy/OATP-SH4	1	0.8	9.21
PPy/OATP-SH5	1	1	11.52

[a] The molar ratio of HCl and SA.

Measurement of Conductivity

For the measurement of conductivity, all test samples were prepared in pellet form (diameter: 13 mm, thickness: 0.6 mm) at a pressure of 40 MPa. Four probes method was used to measure the conductivity of the obtained sample by a four-probe resistivity/square resistance tester (Kund Technology, Guangzhou, China).

Characterizations

The specific surface area, pore size distribution, and micropore volume of ATP and acid-treated ATP were estimated from nitrogen desorption isotherm obtained using a constant-volume adsorption apparatus (ASAP-2020, Micromeritics, USA). Micromorphology of samples was observed by a JSM-6701F field emission scanning electron microscopy (SEM) and an H-8110 transmission electron microscopy (TEM, Hitachi, Tokyo, Japan). The molecular structure of the composite was identified by IR spectroscopy on a Nicolet AVTAR 360 FT-IR using KBr pellets, X-ray photoelectron spectroscopy (XPS, PHI-5000, Perkin-Elmer, USA) and UV-Visible diffuse reflectance study (UV-vis DRS, lambda750, Perkin-Elmer, USA). XRD analysis was conducted on a powder diffractometer (Shimadzu-XRD6000) with CuKα radiation. The thermal property of the composite was observed by Mettler Toledo TGA/DSC1 STARe System.

RESULTS AND DISCUSSION

Structure Characterization

Figure 1 shows the N_2 adsorption–desorption isotherms and pore distributions of ATP and acid-treated ATP. ATP as well as acid-treated ATP exhibit type IV nitrogen adsorption isotherm.[17] After acid treating, the amount of N_2 adsorbed on the ATP is higher than that of the untreated ATP [Figure 1(a)]. Evidently, the pore size of acid-treated ATP is higher than that of untreated ATP, which is mainly distributed in 2–50 nm [Figure 1(b)]. The specific surface area and micropore volume of acid-treated ATP are 175.9 $m^2\ g^{-1}$ and 0.49 $cm^3\ g^{-1}$ (Table IV), respectively. Both of them are slightly larger than that of untreated ATP. These results suggested that the acid-treated ATP is benefit for preparation of organic/inorganic composites than untreated ATP because of its high specific surface area and so on.

Table IV. The Specific Surface Area, Pore Width and Micropore Volume of Acid-Treated ATP and Untreated ATP

Samples	S_{BET} [$m^2\ g^{-1}$][a]	D_{BJH} [nm][b]	V_{BJH} [$cm^3\ g^{-1}$][b]
Acid-treated ATP	175.9	9.5	0.49
Untreated ATP	158.6	6.1	0.32

[a] The specific surface area calculated using the BET equation.
[b] The pore width and micropore volume calculated according to the BJH method.

Figure 2(a) shows XRD of ATP and OATP4, the peak positions of ATP at $2\theta = 8.24°$, 19.72°, and 26.54° corresponded to the primary diffraction of (110), (040), and (400) planes, respectively.[18] And the characteristic peaks of OATP4 are exactly the same as those of ATP, which indicates the ATP crystal is not changed after self-assembly of CPC molecules. The only broad characteristic peak of PPy at about $2\theta = 21.8°$ exhibits that pure PPy is amorphous [Figure 2(b)].[19] By comparison, in PPy/OATP-SH3 samples, the main peaks are similar to those in OATP4 samples, apart from the decreased characteristic peak intensity. An exception only is that the peak intensity of peak position is 20.66° (which is corresponded to the primary diffraction of (121) plane[20]) is enhanced. This is contributed to the fact that the amorphous PPy firmly attaches to the surface of OATP4 and forms the core-shell structures.

According to the FTIR spectra of ATP and OATP4 [Figure 2(c)], the peaks at 1024 and 985 cm^{-1} are corresponding to the stretching vibration of (Mg, Al)-Si-O unite and Si-O-Si(Al) unite, respectively; the peaks at 3553 and 1656 cm^{-1} are attributed to -OH stretching and bending, respectively.[21] In addition, it is notable that two new peaks appear at 2935 and 2843 cm^{-1}

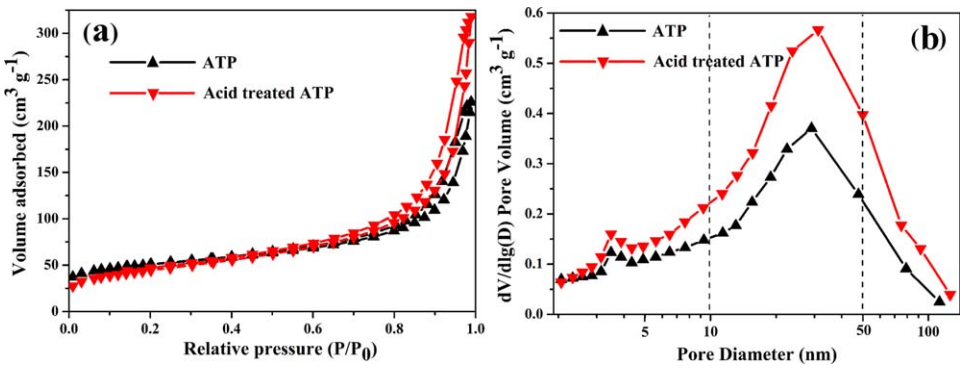

Figure 1. (a) N_2 adsorption-desorption isotherms and (b) pore size distributions of the ATP and acid-treated ATP. [Color figure can be viewed in the online issue, which is available at wileyonlinelibrary.com.]

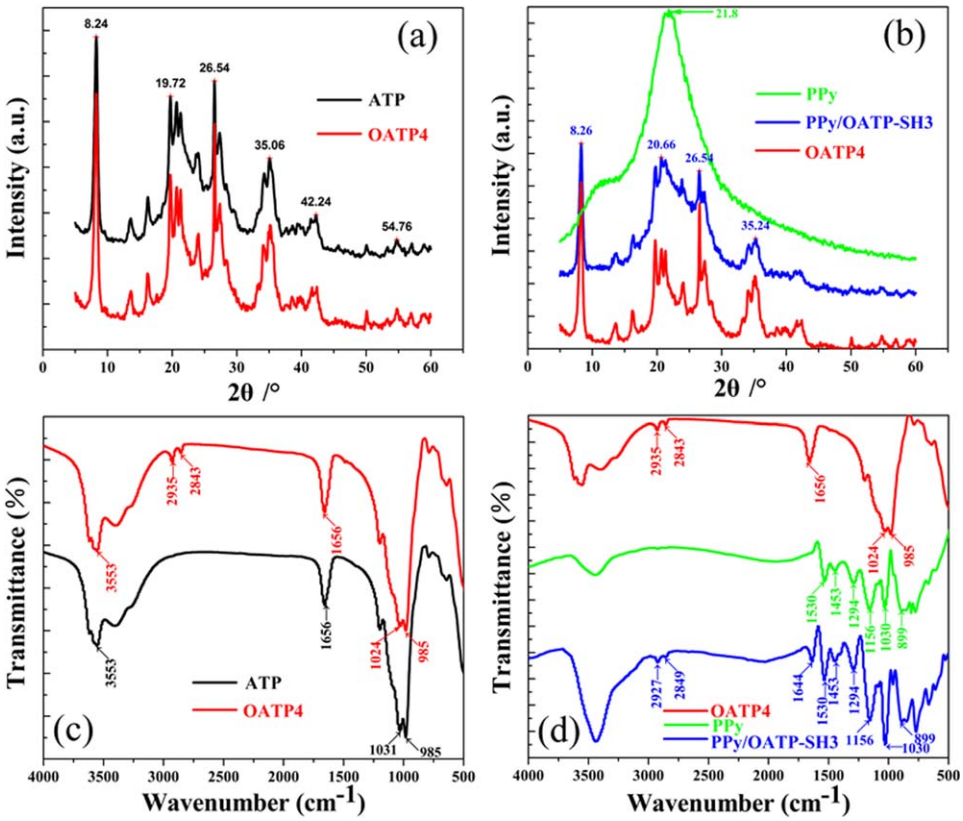

Figure 2. (a) XRD patterns for ATP and OATP4; (b) XRD patterns for PPy, PPy/OATP-SH3, and OATP4; (c) FTIR spectra of ATP and OATP4; (d) FTIR spectra of PPy, PPy/OATO-SH3, and OATP4 (investigated samples in this figure: ATP is original ATP under calcined and acid-treated sample; OATP4 is organic modified ATP, whose preparation conditions is shown in Table I; PPy/OATP-SH3 is HCl secondary doped PPy/OATP composites, whose preparation conditions is shown in Table III). [Color figure can be viewed in the online issue, which is available at wileyonlinelibrary.com.]

in OATP4 samples, which correspond to asymmetrical stretching vibration and symmetrical stretching vibration of -CH_2 unite, respectively. This is a typical illustration for the successful self-assembly of CPC molecules on the surface of ATP. In the IR spectrum of PPy [Figure 2(d)], the peak at 1530 cm^{-1} is for C=C stretching; that at 1453 cm^{-1} is for C-C stretching; the peaks at 1294 and 1030 cm^{-1} may correspond to =C-H band in plane vibration; the peak at 1156 cm^{-1} may be assigned for N-C stretching band; the peak at 899 cm^{-1} may be assigned to the =C-H out of plane vibration indicating polymerization of pyrrole. The above characteristic peaks of PPy are all reflected in the spectrum of the PPy/OATP-SH3 composite [Figure 2(d)]. As a result, it can be proved that the backbone structure of PPy is not damaged by the introduction of OATP. In addition, it is noted that three new peaks appear at 2927, 2849, and 1644 cm^{-1} in PPy/OATP sample, which assigned to typical peaks of OATP. This is a further evidence of PPy chains covered on the surface of OATP4.

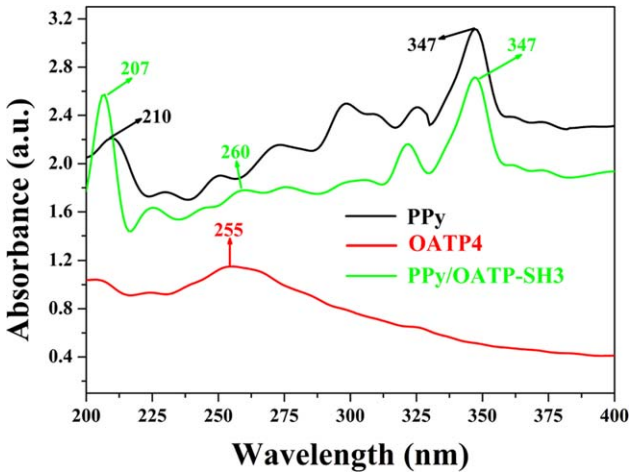

Figure 3. UV-visible diffuse reflectance study of PPy, OATP4, and PPy/OATP-SH3. [Color figure can be viewed in the online issue, which is available at wileyonlinelibrary.com.]

We also performed UV-vis DRS on OATP4, PPy, and PPy/OATP-SH3 (Figure 3). In the UV-vis spectra of PPy, the peak at 210 nm is for π electronic transition in conjugated π bond; the peak at 347 nm is for lone pair of electrons transition in nitrogen atom.[22] For OATP4, the only broad characteristic peak appears at about 255 nm, which is because of Fe^{3+} ions in octahedral coordination. When PPy combined with OATP, the main peaks were similar to those in PPy, but we could find a new peak appeared at 260 nm, which is because of the introduction of OATP4. This is the evidence that PPy chain coated on the surface of OATP and formed the core-shell structure.

To study the formation mechanism of PPy/OATP composites, we performed XPS on PPy and PPy/OATP-SH3, and the results shown

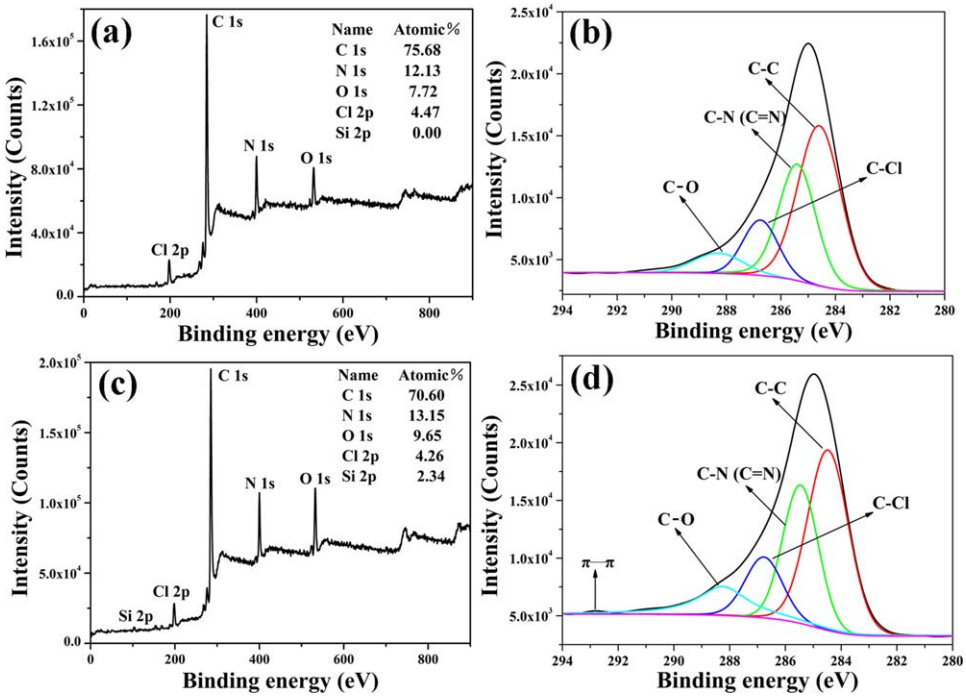

Figure 4. XPS spectra of (a, b) PPy and (c, d) PPy/OATP-SH3. [Color figure can be viewed in the online issue, which is available at wileyonlinelibrary.com.]

in Figure 4. Compared with PPy [Figure 4(a)] and PPy/OATP-SH3 [Figure 4(c)], the amount of silicon and oxygen atoms in PPy/OATP-SH3 is higher than those in PPy, because of the introduction of OATP. For PPy, the XPS peaks of C 1s in Figure 4(b) are reasonably decomposed into four Gaussian peaks with binding energies of 284.6 (C-C), 285.4 (C-N/C=N), 286.7 (C-Cl), and 288.4 eV (C-O),[22] respectively. When combined with OATP, the main peaks were similar to those in PPy samples [Figure 4(d)]. However, it is worth noting that a small peak centered at 292.8 eV was observed in Figure 4(d), which is assigned to π–π stacking effect between PPy and the CPC molecules on the surface of OATP.[23]

Figure 5(a) shows TGA curve comparison of ATP and OATP4. The first mass loss of ATP occurs at room temperature to 98.8°C, which is attributed to the loss of adsorbed water. The second mass loss of ATP occurs at 98.8–219.3°C, which is ascribed to the loss of hydration water. A platform is observed at 219.3°C to 318.8°C and then the subsequent mass loss of ATP is ascribed to the coordination water.[24] In OATP4 TGA curve, the platform at 219.3°C to 318.8°C was disappeared and a mass loss of this range gives rise to the CPC molecules degradation. This is further evidence on successful self-assembly of CPC molecules on ATP surfaces. TGA curves of OATP4, PPy, and PPy/OATP-SH3 composites in Figure 5(b) exhibit that: the thermal degradation of the PPy sample occurs at 163.84°C, while, in PPy/OATP-SH3 sample, the thermal degradation of PPy occurs at 249.29°C. This shows that thermal stability of composites is enhanced and it can be attributed to the retardation effect of OATP as barriers for the degradation of PPy.[16,25]

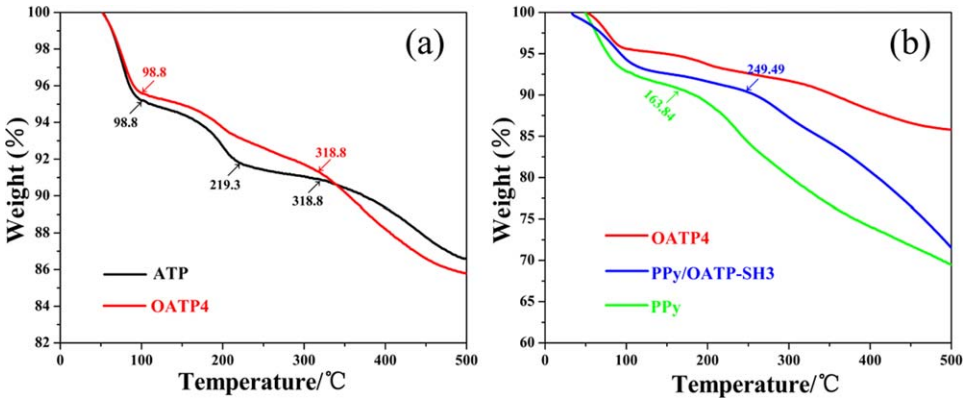

Figure 5. (a) TGA patterns of ATP and OATP4 and (b) TGA patterns of PPy, PPy/OATP-SH3, and OATP4. [Color figure can be viewed in the online issue, which is available at wileyonlinelibrary.com.]

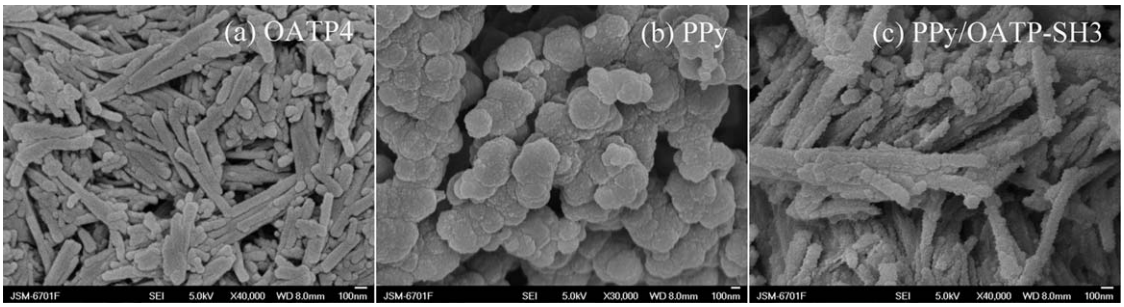

Figure 6. SEM images of (a) OATP4, (b) PPy, and (c) PPy/OATP-SH3.

Figures 6 and 7 show the micro-morphology of OATP4, PPy, and PPy/OATP-SH3. As shown in Figures 6(a) and 7(a), OATP4 nanoparticles exhibit a rod-like structure; the diameter and length are approximately 22–30 nm and 400–800 nm, respectively. In addition, the surface of OATP4 is smooth [Figure 6(a)] and crossed with each other to form the spliced network [Figure 7(a)]. PPy nanoparticles are basically spherical [Figure 6(b)] and form agglomerates [Figure 7(b)], whose range between 100 and 300 nm. PPy/OATP-SH3 composite are also rod-like, whose diameter are approximately 90–120 nm, larger than those of OATP4 [Figure 7(c)]; the surface of PPy/OATP-SH3 is not smooth but like fish scales [Figure 6(c)]. This evidences that OATP4 nanoparticles are well covered by spherical PPy, forming core-shell structures [see Figure 7(c), the arrows indicate the PPy layer on the surface of OATP4]. Meanwhile, the PPy/OATP-SH3 nanoparticles cross with each other to form the conductive spliced network [see Figure 7(c), in circle] and these benefit for the conductivity improvement of composites.

Formation Mechanism of PPy/OATP Composites

Scheme 1 demonstrates the proposed possible formation process of PPy/OATP composites. This process includes three steps: firstly, ATP is modified by CPC molecules through the hydrogen-bonding interactions between pyridine rings and hydroxyl on the surface of ATP to get OATP powder[26]; secondly, OATP powder is stably dispersed in water by magnetic stirring, and then a large amount of Py is added to the suspension, when Py molecules combine with pyridine rings of CPC molecule via π–π stacking interaction on the surface of OATP; finally, as the oxidant $FeCl_3$ added, the polymerization process happens on the surface of ATP and PPy chains firmly attach to the surface of ATP. As a result, crystallite structure of PPy/OATP is similar to OATP.

Conductivity of Composites

The effect of CPC amount on the conductivity of the PPy/OATP-S composites is plotted in Figure 8(a). With the increase of CPC, the conductivity first increases and then decreases sharply, peaking at 75.18 S cm^{-1} when the mass ratio of CPC/ATP maintains to 0.03 (OATP4 sample). To explain this, we suppose that Py monomers are adsorbed on OAPT surface by π–π stacking interaction between the terminal pyridine groups of OATP surface and Py monomers. The condensed concentration of reactant on the surface of OAPT facilitates the formation of short oligomers in the initiation step of polymerization. As we all know, short oligomers in initiation step could serve as reaction initiation centers[27–29] and the pre-alignment of monomers on OATP promotes the backbone growth of PPy in the propagation step of the polymerization. So, with the increase of CPC amount, the conductivity of PPy increases initially. However, when the mass ratio of CPC/ATP is larger than 0.03, the absorbed monomers probably form too much oligomers in the initiation step, which restrains the growth of longer polymer backbone.

The influence of OATP4 amount on the conductivity of PPy/OATP-S composites is shown in Figure 8(b). It can be found that with the increase in the OATP4 amount, the conductivity first increases and then decreases as well. However, the conductivity of PPy/OATP-S composites are much higher than that of pure PPy (23.1 S cm^{-1}). When the mass ratio of OATP4/Py reached to 0.6 (PPy/OATP-S2 sample), the conductivity of composites shows the maximum value of 75.18 S cm^{-1}. The total conductivity of the composites may depend on two aspects: the first one is the intrinsic properties of conducting polymer (PPy), such as doping level, conjugation length, and chain length; as the counterpart, the inhomogeneities, compactness,

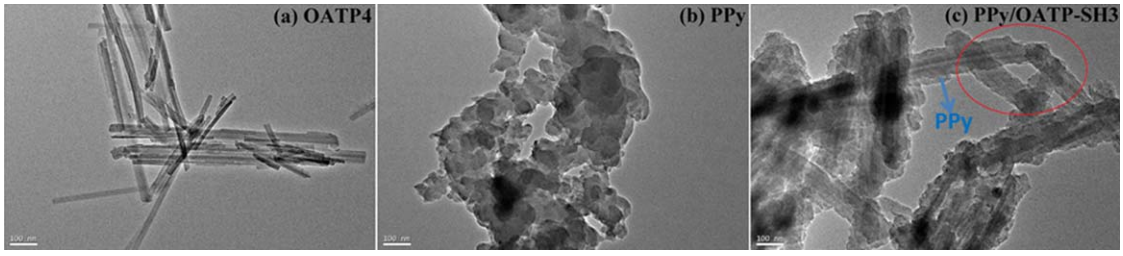

Figure 7. TEM images of (a) OATP4, (b) PPy, and (c) PPy/OATP-SH3. [Color figure can be viewed in the online issue, which is available at wileyonlinelibrary.com.]

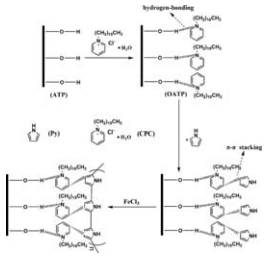

Scheme 1. Proposed possible formation process of PPy/OATP composites.

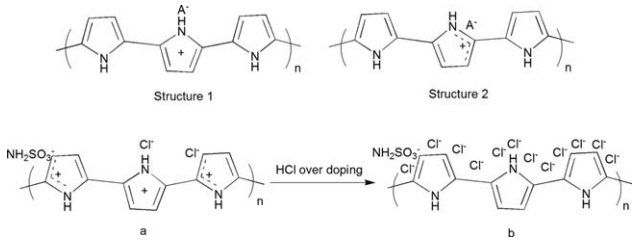

Figure 9. Counter-anions doping (structure 1); Proton-acid doping (structure 2). (a) The structure of PPy chain by HCl secondary doping; and (b) The structure of PPy chain by secondary overdoping of HCl.

and orientation of composites also play important roles on conductivity value.[30] Since the PPy/OATP composites are inhomogeneous, compactness, and molecular orientations may significantly vary because of the variation in the amount of OATP in the composites. We suppose that the nano-rod structured OATP4 may give rise to the increase of the composites' orderings (confirmed from XRD), which increases the compactness and molecular orientations, and hence results in an increase of conductivity.

Pure PPy is very light with poor compactness. The microparticles are randomly oriented and the linkage among the polymer particles through the grain boundaries is very weak, leading to relatively lower conductivity.[31] Considering that compactness of OATP4 is higher than that of PPy, we suppose the presence of OATP4 in the composites results in an improvement in the compactness of the composite material. On the other hand, the regular growth of PPy chains on the surface of OATP4 matrix connects each other to form a conducting network with low contact resistance. This structure can effectively avoid weak bonding. Therefore, the conductivity of PPy/OATP-S composites is much higher than that of pure PPy. However, if the amount of OATP4 continues to increase, the PPy chains could not form continuous network anymore. In this case, the conductivity of the composites mainly depends on the insulated nature of OATP4, thereby decreasing the conductivity of composites.

The impact of HCl amount on the conductivity of PPy/OATP-SH composites is shown in Figure 8(c). The conductivity increases with the increase of HCl amount firstly. When the molar ratio of HCl/SA reaches to 0.5 (PPy/OATP-SH3 sample) the conductivity of composites shows the maximum value like 87.59 S cm^{-1}. Beyond the molar ratio of 0.3, the conductivity decreases sharply.

Li et al.[32,33] proposed that there are two doping structures for PPy-based composites: oxidized conjugated chain doped with counter-anions (Figure 9, structure 1) and proton-acid doping structure (Figure 9, structure 2). Structure 1 is widely verified in literatures, but structure 2 is rarely reported.[33] In structure 2, it is assumed that β-C of pyrrole unit is protonated and the PPy chain is doped by the deprotonation structure.[32] $FeCl_3$ serves as not only a kind of oxidant but also a kind of dopant, which carries out counter-anions doping. Based on proton-acid doping principle, after the protonation of β-C in pyrrole unit, the PPy chain will be doped by the deprotonated structure, and simultaneously, the negative ions will be doped in PPy chains to maintain the charge balance. SA as the dopant carries out proton-acid doping and its negative ions ($NH_2SO_3^-$) have a large molecular size. If SA is doped in PPy chains, the PPy chains will be stretched strongly because of the negative ions according Titelman's report.[34] We suppose that this phenomenon benefits for the secondary doping by small molecule acid and which is called the "size memory effect",[35] such as HCl [Figure 9(a)]. This will explain why the conductivity of composites increases with the increase of HCl at the initial stage. However, excessive HCl makes too much negative ions encapsulated in PPy chains [Figure 9(b)], leading to instability of conjugated chains induced from repulsion force. In this case, electron conduction is blocked and the conductivity of composites decreases.[10]

CONCLUSIONS

In summary, we report a facile and effective method for synthesizing secondary doped PPy/OATP composites (first doped by SA and secondary doped by HCl). Compared the sample only

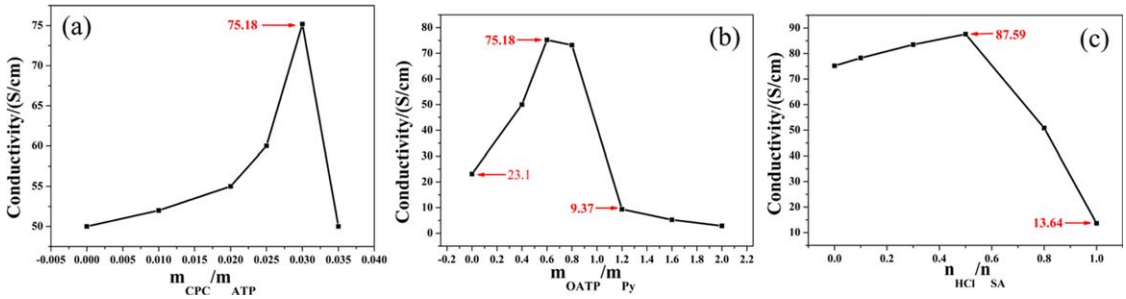

Figure 8. Conductivities of samples at room temperature. (a) The effect of CPC amount on the conductivity of the PPy/OATP-S composites; (b) the influence of OATP4 amount on the conductivity of PPy/OATP-S composites; and (c) the influence of HCl amount on the conductivity of PPy/OATP-SH composites. [Color figure can be viewed in the online issue, which is available at wileyonlinelibrary.com.]

doped once, the secondary doped PPy/OATP samples have larger conductivity of 87.59 S cm^{-1} and also higher thermal degradation temperature of 249.29°C. These composites possess unique core-shell three-dimensional structures, high conductivity, as well as excellent thermal stability, allowing their applications in anti-corrosion coating,[36] shielding of electromagnetic interferences,[37] and many other areas.[38]

ACKNOWLEDGMENTS

This work was financially supported by the National Natural Science Foundation of China (No.51063003) and the Fundamental Research Funds for the Universities of Gansu (No.1105ZTC136).

REFERENCES

1. Kumar, A.; Singh, R. K.; Agarwal, K.; Singh, H. K.; Srivastava, P.; Singh, R. *J. Appl. Polym. Sci.* **2013**, *130*, 434.
2. Park, K. H.; Jo, E. A.; Na, K. *Biotechnol. Bioproc. E* **2007**, *12*, 463.
3. Li, J.; Wei, W. Z.; Luo, S. L. *Microchim. Acta* **2010**, *171*, 109.
4. Kim, D. Y.; Lee, J. Y.; Kim, C. Y.; Kang, E. T.; Tan, K. L. *Synth. Met.* **1995**, *72*, 243.
5. Curtin, L. S.; McEllistrem, M.; Pietro, W. J. *J. Phys. Chem.* **1989**, *93*, 1637.
6. Bay, L.; Mogensen, N.; Skaarup, S.; Sommer-Larsen, P.; Jorgensen, M.; West, K. *Macromolecules* **2002**, *35*, 9345.
7. Nalwa, H. S. *J. Mater. Sci.* **1992**, *27*, 210.
8. He, C.; Yang, C.; Li, Y. F. *Synth. Met.* **2003**, *139*, 539.
9. Kim, J. W.; Liu, F.; Choi, H. J.; Hong, S. H.; Joo, J. *Polymer* **2003**, *44*, 289.
10. Tang, Q. W.; Sun, X. M.; Li, Q. H.; Lin, J. M.; Wu, J. H. *J. Mater. Sci.* **2009**, *44*, 849.
11. Ramesan, M. T. *J. Appl. Polym. Sci.* **2013**, *128*, 1540.
12. Rashidzadeh, Olad, A.; Ahmadi, S. *Polym. Eng. Sci.* **2013**, *53*, 970.
13. Dubey, N.; Leclerc, M. *Polym. Phys.* **2011**, *49*, 467.
14. Mallouki, M.; Tran-Van, F.; Sarrazin, C.; Simon, P.; Daffos, B.; Fauvarque, J. *J. Solid State Electrochem.* **2007**, *11*, 398.
15. Chen, J. C.; Wang, H. D.; Luo, W. Q.; Xiang, J. M.; Zhang, L. H.; Sun, B. B. *Colloid Polym. Sci.* **2010**, *288*, 173.
16. Yang, C.; Liu, P. *Synth. Met.* **2009**, *159*, 2056.
17. Nishiyama, N.; Zheng, T.; Yamane, Y.; Egashira, Y.; Ueyama, K. *Carbon* **2005**, *43*, 269.
18. Zhang, S. S.; He, P.; Lei, W.; Zhang, G. L. *J. Electroanal. Chem.* **2014**, *724*, 29.
19. Liu, J.; Wan, M. X. *J. Mater. Chem.* **2001**, *11*, 404.
20. Nan, F.; Xu, Y.; Xu, B. S.; Gao, F.; Wu, Y. X.; Tang, X. H. *Appl. Surf. Sci.* **2014**, *307*, 86.
21. Hu, T.; Tan, L. Q. *J. Radioanal. Nucl. Chem.* **2012**, *292*, 819.
22. Wang, H. L.; Hao, Q. L.; Yang, X. J.; Lu, L. D.; Wang, X. *ACS Appl. Mater. Interfaces* **2010**, *2*, 821.
23. Fan, X. B.; Peng, W. C.; Li, Y.; Li, X. Y.; Wang, S. L.; Zhang, G. L.; Zhang, F. B. *Adv. Mater.* **2008**, *20*, 4490.
24. Vágvölgyi, V.; Daniel, L. M.; Pinto, C.; Kristóf, J.; Frost, R. L.; Horváth, E. *J. Therm. Anal. Calorim.* **2008**, *92*, 589.
25. Choi, J. S.; Sung, J. H.; Choi, H. J.; Jhon, M. S. *Synth. Met.* **2005**, *153*, 129.
26. Wan, Y.; Shi, Y. F.; Zhao, D. Y. *Chem. Mater.* **2008**, *20*, 932.
27. Wang, Y.; Tran, H. D.; Kaner, R. B. *Macromol. Rapid Commun.* **2011**, *32*, 35.
28. Stejskal, J.; Sapurina, I.; Trchová, M. *Prog. Polym. Sci.* **2010**, *35*, 1420.
29. Tan, L.; Wang, B.; Feng, H. X. *RSC Adv.* **2013**, *3*, 2561.
30. Chen, G. Z.; Shaffer, M. S. P.; Coleby, D.; Dixon, G.; Zhou, W.; Fray, D. J.; Windle, A. H. *Adv. Mater.* **2000**, *12*, 522.
31. Gangopadhyay, R.; De, A. *Eur. Polym. J.* **1999**, *35*, 1985.
32. Li, Y. F.; Ouyang, J. Y.; Yang, J. *Synth. Met.* **1995**, *74*, 49.
33. Li, Y. F.; He, G. F. *Synth. Met.* **1998**, *94*, 127.
34. Titelman, G. I.; Siegmann, A.; Narkis, M.; Wei, Y. *J. Appl. Polym. Sci.* **1998**, *69*, 2205.
35. Abd-Elwahed, Holze, R. *Synth. Met.* **2002**, *131*, 61.
36. Castagno, K. R. L.; Dalmoro, V.; Mauler, R. S.; Azambuja, D. S. *J. Polym. Res.* **2010**, *17*, 647.
37. Geetha, S.; Satheesh Kumar, K. K.; Rao, C. R. K.; Vijayan, M.; Trivedi, D. C. *J. Appl. Polym. Sci.* **2009**, *112*, 2073.
38. Geetha, S.; Rao, C. R. K.; Vijayan, M.; Trivedi, D. C. *Anal. Chim. Acta* **2006**, *568*, 119.